Asian Journal of Chemistry; Vol. 34, No. 6 (2022), 1425-1430

ASIAN JOURNAL OF CHEMISTRY

https://doi.org/10.14233/ajchem.2022.23639

Thermal Studies of Aqueous Free-Base Porphyrin and Metalloporphyrins of Cu, Ag and Mn

S.D. GOKAKAKAR[1,*] and A.V. SALKER[2]

[1]P.E.S.'s R.S.N. College of Arts and Science, Farmagudi, Ponda, Goa-403401, India
[2]School of Chemical Sciences, Goa University, Goa-403206, India

*Corresponding author: E-mail: sdgokakakar@gmail.com

Received: 26 November 2021; *Accepted*: 17 February 2022; *Published online*: 18 May 2022; AJC-20801

Present study is intended on the thermal behaviour of the free base aqueous porphyrin and the corresponding metalloporphyrins of some of the transition metal ions such as Cu, Ag and Mn. The respective porphyrins were synthesized and characterized by ultra violet-visible spectroscopy, infrared spectroscopy and high-resolution mass spectrometry. These porphyrins thus obtained were then subjected to thermal analysis from room temperature to 800 ºC. It was observed that free-base porphyrin tetrasodium *meso*-tetra (*p*-sulphonatophenyl) porphyrin ($TPPS_4$) is stable up to 360 ºC and remaining metalloporphyrins are stable in the range of 435-460 ºC, respectively. Further, the hygroscopic porphyrins were subjected to fixation of number of water molecules of crystallization and quantitative analysis with respect to % of metal oxide, % of Na^+, % SO_4^{2-} and % coal respectively.

Keywords: Aqueous-porphyrins, Thermogravimetry, Differential scanning calorimetry, Relative thermal stabilities.

INTRODUCTION

The research in the last three decades has proved that the practical applications of porphyrins in the medicals, where drug delivery is focussed and other areas where clinical studies have incorporated bio-imaging or bio-sensing as the most reliable advanced techniques [1]. The porphyrins are basically metal-organic compounds with adjustable porous structures; therefore, they possess very high drug loading capacity and biodegradability. Due to these properties of porphyrins the delivery of the drugs can be maintained at the controlled rate in various therapeutic applications. The use of metalloporphyrins in drug-delivery may be explored in the administration of drug-doses and other side effects due to unlocalized distribution of drug [2-4]. It is to be worth noting that the various types of bonds between porphyrins and drug molecules such as hydrogen bonding, van der Waal's interactions or other hydrophobic interactions are responsible in releasing drug from the metallo-porphyrins depending upon the stimuli-response. In this regard temperature and pH are helpful in controlling the release-rate of the drug [5,6].

The porphyrins are being extensively used as theragnostic agents where a combination of therapeutics and diagnostics is used in MRI, photodynamic cancer therapy (PDT) and single cell imaging [7-10]. MRI is useful in the visualization of the human body. This is a non-invasive *in vivo* technology and considered to be the most reliable imaging technique [11,12]. The porphyrins are extensively used as contrasting agents in MRI for the localization of tumour [13-15]. In actual practice, there are variety of clinically-approved contrast agents, but to treat malignant neoplastic diseases hardly they are available commercially. This has made to focus more attention on the use of porphyrins and metalloporphyrins [16-18]. Therefore, it essential to have compatibility of size of the metal and porphyrin cavity for highly stable chelates for the application *in vivo* imaging techniques. The molecules of porphyrins are looked upon as having multiple functionalities with the high tissue penetrating power.

It is a documented fact that 15% of the death in the entire globe are caused due to cancer [19,20]. The growth of the abnormal cells in the body is a consequence of several factors such as weakness of immune system, harmful radiations, some typical chemicals and inherited mutations [21,22]. In photo dynamic therapy (PDT), the porphyrins are widely used because they have unique affinity for tumour tissues on account of their photosensitizing property. In addition, they are also good

carriers to transport other active drugs into tumour tissues. Unlike other cancer therapies, PDT is non-toxic and slightly-invasive, therefore, it can be applied to the places where surgery is not possible. The range of applications of PDT can be extended to oncology, cardiovascular diseases and other infectious diseases.

The inherent macrocyclic structure of free-base porphyrin and metalloporphyrins makes it suitable for clinical studies including chemo sensors [23,24]. In recent past, it is also evidenced that the synthetic porphyrins play an important role in the disease treatment as a promising candidate with respect to their photochemical, biological and photo physical properties [25]. Besides this, they also find applications in photocatalysis [26,27], molecular photovoltaics [28] and non-linear optics [29].

In present study, the relative thermal stabilities of the synthesized porphyrins are investigated and the subsequent decomposition temperatures in synthetic air, the fixation of water of crystallization molecules and the quantitative analysis of the residue remaining after TG-DSC operation.

EXPERIMENTAL

Tetraphenyl porphyrin (TPP), a precursor, was used for the synthesis of aqueous free-base porphyrin tetrasodium *meso*-tetra(*p*-sulphonatophenyl) porphyrin ($TPPS_4$) [30]. Vacuum dried TPP and conc. H_2SO_4 in the molar ratio 0.003: 0.5 were refluxed in a flask for 8 h and the entire reaction mixture was kept undisturbed for next 48 h. Further, the distilled water followed by lime was added to the reaction mixture to attain the purple colour. The byproduct $CaSO_4$ was removed and pH of the solution was adjusted to 8-10 by the addition of Na_2CO_3. The next step was removal of $CaCO_3$ precipitate and subsequent addition of ethyl alcohol as per requirement. This filtrate was concentrated on a steam bath and was dried in an oven at 100 ºC for continuous 2 h. The crystals of $TPPS_4$ are nearly deliquescent in nature, therefore, kept in an air tight container. They were further purified by dry column chromatography, where stationary phase was basic alumina and the mobile phase was a mixture of water, methanol and acetone in the ratio 7:2:1. Out of different bands developed on the column, only purple coloured band, which was due to $TPPS_4$ was selected and another green coloured band due to dication was rejected. Every time $TPPS_4$ was vacuum dried and used for subsequent preparation of metalloporphyrins.

The synthesis of metalloporphyrins was carried out by introducing the metals such as Cu, Ag and Mn, in the porphyrin moiety by standard method. The respective metalloporphyrins were synthesized by refluxing the corresponding salt of the metal with aqueous solution of $TPPS_4$ for 0.5 h. The reaction was not proceeding as per the stoichiometric proportion therefore, two fold or sometimes more salt was required for the completion of the reaction to get $CuTPPS_4$ [tetrasodium meso-tetra (*p*-sulphonatophenyl) porphinatocopper(II)], $AgTPPS_4$ [tetrasodium *meso*-tetra(*p*-sulphonatophenyl)porphinato silver(II)] and $MnTPPS_4Cl$ [tetrasodium *meso*-tetra(*p*-sulphonatophenyl)porphinatomanganese(III) chloride], respectively. All of them were purified by dry column chromatography with stationary and mobile phases as mentioned above. The yield of the metalloporphyrins after purification was found to be about 80-85%.

The ultraviolet-visible spectra were recorded using Shimadzu spectrophotometer (model UV/2450UV) for 10^{-5} M concentration. The infrared spectra were recorded on Shimadzu IR spectrometer (model prestige/21FTIR). The high-resolution mass spectrum for $TPPS_4$ was recorded using (model Varian 500-MS) and the respective mass of the compound was calculated. The thermal analysis of these compounds was carried out using NETZSCH-Geratbau Gmbh thermal analyser (STA 409PC) from room temperature to 800 ºC.

RESULTS AND DISCUSSION

UV-visible studies: The porphyrins are chromophoric compounds, where they absorb strongly in UV as well as visible regions. There are two types absorption bands obtained *viz,* Soret bands and Q bands, respectively. Soret bands are very intensive in the range 394-422 nm, which is a special property of porphyrins. Fig. 1 shows overlay of above porphyrins, where the Soret bands are for $TPPS_4$ (413 nm), $CuTPPS_4$ (412 nm), $AgTPPS_4$ (422 nm) and $MnTPPS_4Cl$ (413 nm), respectively as observed for 10^{-5} M concentration. These are in good agreement with the literature values [31,32]. They also give less intense Q-bands in the visible region, where, with the introduction of metal in the porphyrin hole, some bands disappear and confirm the formation respective metalloporphyrin.

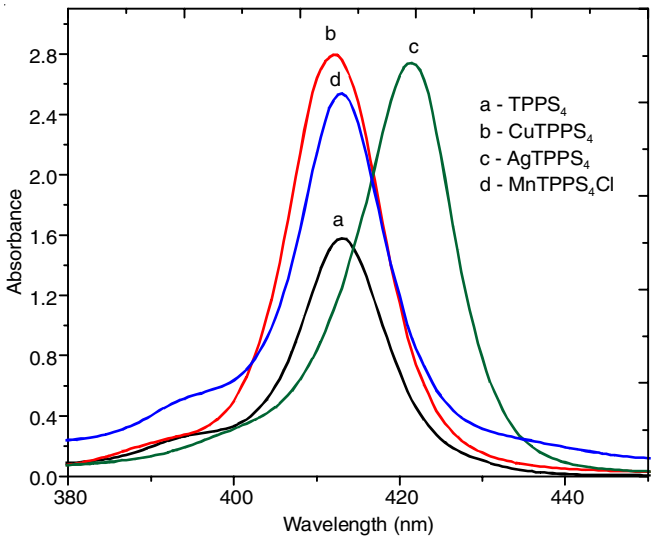

Fig. 1. Overlay of porphyrins for intense Soret band for 10^{-5} M concentration

Infrared studies: The difference between non-aqueous and aqueous porphyrins is that in latter case there is substitution of SO_3Na group at *para*-position of four phenyl rings to make it an aqueous-porphyrin. The characteristic stretching frequencies for the substitution of SO_3Na group are $TPPS_4$ (1184, 1128 and 1041cm^{-1}), $CuTPPS_4$ (1184, 1130 and 1041 cm^{-1}), $AgTPPS_4$ (1186, 1130 and 1041 cm^{-1}) and $MnTPPS_4Cl$ (1192, 1128, 1041 cm^{-1}), respectively. Fig. 2 shows the characteristic peaks for O-H (water of crystallization) and C-H (pyrrole) stretching frequencies at 3523 cm^{-1} and 3120 cm^{-1}. Fig. 3 shows substitution of SO_3Na group in phenyl ring [33].

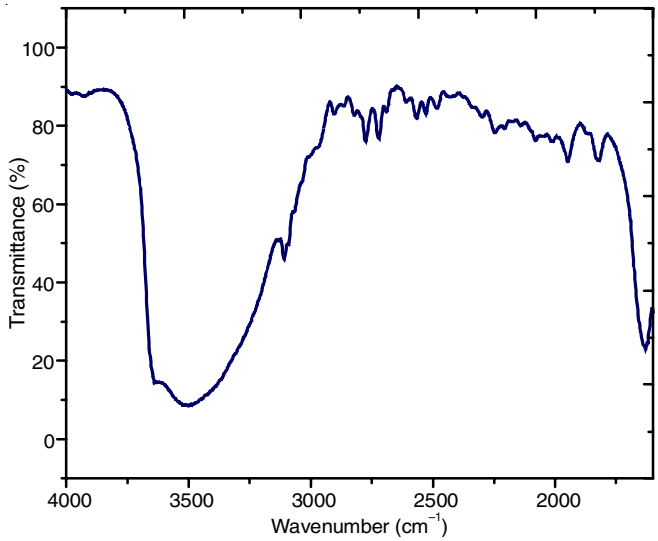

Fig. 2. IR spectra of $AgTPPS_4$ for O-H and C-H stretch

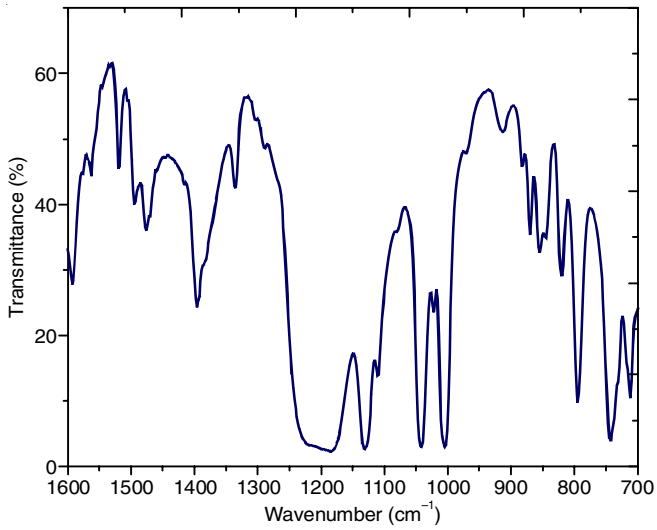

Fig. 3. IR spectra of $AgTPPS_4$ for substitution of SO_3Na group in phenyl ring

High resolution mass spectrometry: As a representative compound of porphyrins, $TPPS_4$ was subjected to high resolution mass spectrometry for the calculation of the molecular weight and confirmed (Fig. 4).

TG/DSC studies: The thermogravimetric and differential scanning calorimetric methods were used to study the various thermal events in porphyrins taking place after the application of heat from room temperature to 800 ºC in synthetic air.

TG/DSC of $TPPS_4$: The TG/DSC curve for $TPPS_4$ is shown in Fig. 5. The weight loss of 7.8% is shown by TG curve and an endothermic peak is shown by DSC curve at 74.5 ºC. Since

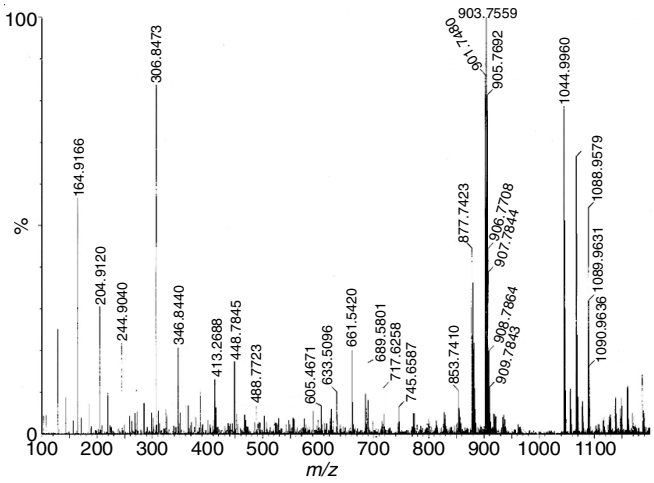

Fig. 4. High resolution mass spectra for molecular weight of $TPPS_4$

the compound is nearly deliquescent, there is a loss of water of crystallization from the compound at this temperature. The number of molecules of water of crystallization for this compound are found to be five, therefore, the molecular formula of compound is deduced as $TPPS_4 \cdot 5H_2O$ (Table-1). Further, there is continuous mass loss and at 350 ºC, the compound starts decomposing as shown by DSC curve. The next decomposition temperatures were observed at 468 and 605 ºC, respectively. After this temperature, the total per cent loss of mass is about 55.5%. Thus, $TPPS_4$ decomposes in three different stages as mentioned above. Therefore, the thermal stability of the compound is up to around 360 ºC.

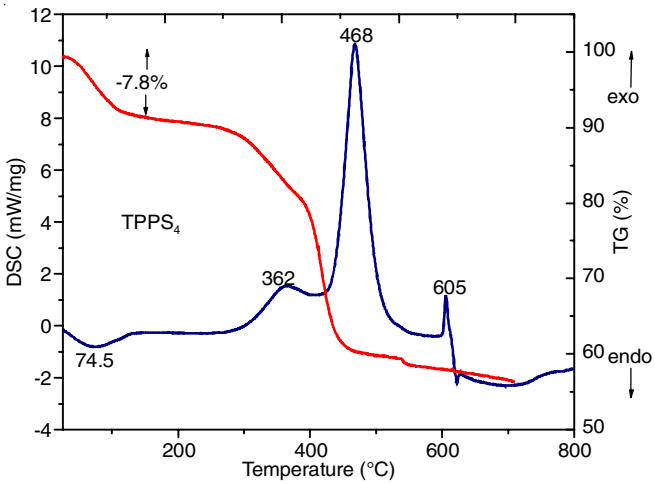

Fig. 5. TG/DSC curve for free-base $TPPS_4$

Analysis of residue: When the residue of $TPPS_4$ after TG/DSC analysis was subjected to qualitative and quantitative

TABLE-1
FIXATION OF WATER OF CRYSTALLIZATION MOLECULES IN AQUEOUS-PORPHYRINS

Porphyrin	Weight taken for TG-DSC (mg)	Loss due to H_2O (%)	Molecular weight of anhydrous compound	Molar ratio	Water of crystallization	Formula
$TPPS_4$	10.000	-7.8	1024	1:5	05	$TPPS_4 \cdot 5H_2O$
$CuTPPS_4$	10.000	-14.11	1087.55	1:10	10	$CuTPPS_4 \cdot 10H_2O$
$AgTPPS_4$	11.400	-13.84	1131.86	1:10	10	$AgTPPS_4 \cdot 10H_2O$
$MnTPPS_4Cl$	10.600	-13.53	1114.39	1:10	10	$MnTPPS_4Cl \cdot 10H_2O$

analysis following results were obtained. The residue showed the presence of Na^+, SO_4^{2-} and coal (porphyrins being aromatic hydrocarbons). It is observed in TG-EGA-MS analysis [34] Na^+ ions are not lost during process because its boiling point is 881 ºC and our limiting temperature is 800 ºC. But in case of SO_3^{2-} group, it seen in TG-EGA-MS analysis that it is lost in many possible ways as S^+, HS^+, H_2S, *etc.* Similarly, it is also observed that in the synthetic air, SO_3^{2-} gets oxidized to SO_4^{2-}, confirmed by confirmative tests in qualitative analysis. Therefore, the amount of SO_4^{2-} should be calculated in the remaining residue after thermal analysis. The results of this calculation are shown in Table-2. In case of $TPPS_4$, it is 8.97% Na^+, 37.49% SO_4^{2-} and 53.53% coal, respectively.

TG/DSC of $CuTPPS_4$: The TG/DSC curve for $CuTPPS_4$ is shown in Fig. 6. The TG curve shows 70% of total loss of compound up to 800 ºC and 14.11% loss is due to the water of crystallization at 72 ºC. The molar ratio of the compound to water is found as 1:10, therefore, the molecular formula can be deduced as $CuTPPS_4 \cdot 10H_2O$ (Table-1). The DSC curve further shows two major decomposition temperature at 462 and 475 ºC, which give substantial evidence for the opening of pyrrole and phenyl rings. This curve confirms the thermal stability of $CuTPPS_4$ at around 375 ºC.

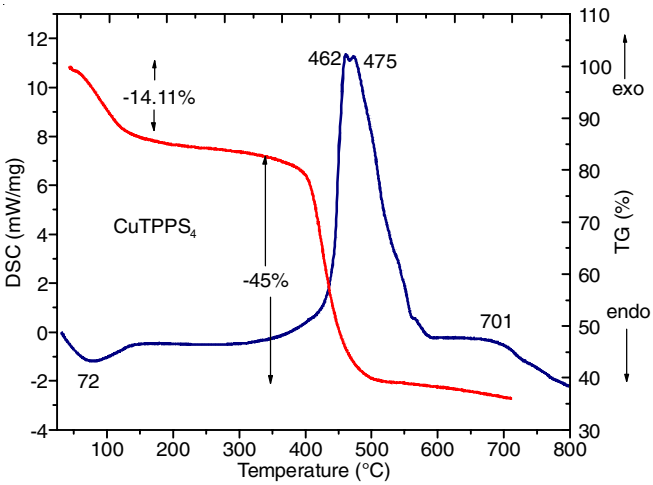

Fig. 6. TG/DSC curve for $CuTPPS_4$

Analysis of residue: After the completion of TG/DSC operation at 800 ºC, the residue was analyzed and following results were obtained as 8.46% Na^+, 35.31% SO_4^{2-}, 48.91% coal and 7.31% metal oxide (Table-2). The magnetic moment revealed that it is low-spin chelate. Therefore, the oxidation state of central metal Cu is expected to be as +2, similarly, the operation was conducted in highly oxidizing synthetic air, therefore, the formation of CuO as a stable oxide is strengthened.

TG/DSC of $AgTPPS_4$: The TG/DSC curve for $AgTPPS_4$ is shown in Fig. 7. The total loss observed for this metalloporphyrin was 70% whereas the loss due to water of crystallization was observed at 85.5 ºC as 13.84%. The molar ratio for this loss was in the ratio 1:10, therefore the molecular formula with water of crystallization for a compound is deduced as $AgTPPS_4 \cdot 10H_2O$. The DSC curve shows three major decomposition temperatures at 450, 548 and 584.7 ºC, which confirms thermal stability up to 350 ºC (from TG curve). The temperatures 450, 548 and 584.7 ºC give the information about the opening of pyrrole ring followed by phenyl rings.

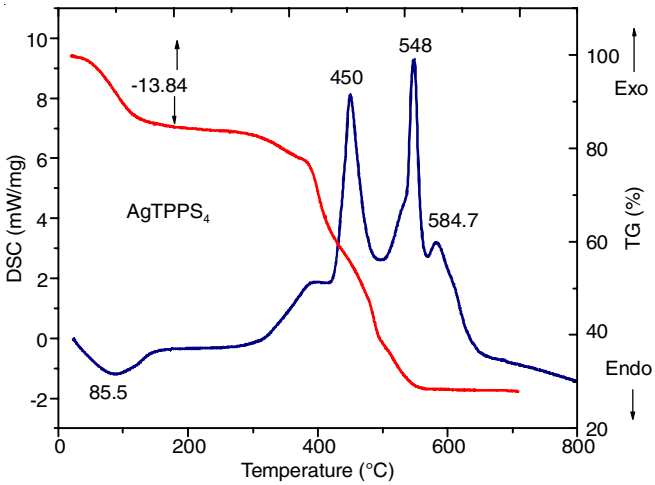

Fig. 7. TG/DSC curve for $AgTPPS_4$

Analysis of residue: The analysis of the residue remaining after the TG/DSC analysis as 8.13% Na^+, 33.92% SO_4^{2-}, 47.71% coal and 10.23% metal oxide (Table-2). In this case, due to oxidizing environment, the most stable oxide of silver *i.e.* Ag_2O is expected.

TG/DSC of $MnTPPS_4Cl$: As shown in Fig. 8, the weight loss due to water is observed at 13.53% at 92.1 ºC. The molar ratio found for this event is 1:10, therefore, the compound can

TABLE-2
QUANTITATIVE ANALYSIS OF RESIDUE OF PORPHYRINS BASED ON TG-DSC MEASUREMENTS

Porphyrin	$TPPS_4$	$CuTPPS_4$	$AgTPPS_4$	$MnTPPS_4Cl$
Wt. of porphyrin (mg)	9.40	10.00	11.40	10.60
Residue remaining (mg)	5.26	3.500	3.19	2.01
Residue loss (mg)	4.14	6.500	8.21	8.59
Amount of Na^+ (mg)	0.47	0.30	0.26	0.17
Na^+ (%)	8.97	8.46	8.13	8.26
Amount of SO_4^{2-} (mg)	1.97	1.24	1.08	0.69
SO_4^{2-} (%)	37.49	35.31	33.92	34.45
Amount of metal oxide (mg)	–	0.26	0.33	0.13
Metal oxide (%)	–	7.31	10.23	6.36
Amount of coal	2.82	1.71	1.52	1.01
Coal (%)	53.53	48.91	47.71	50.42

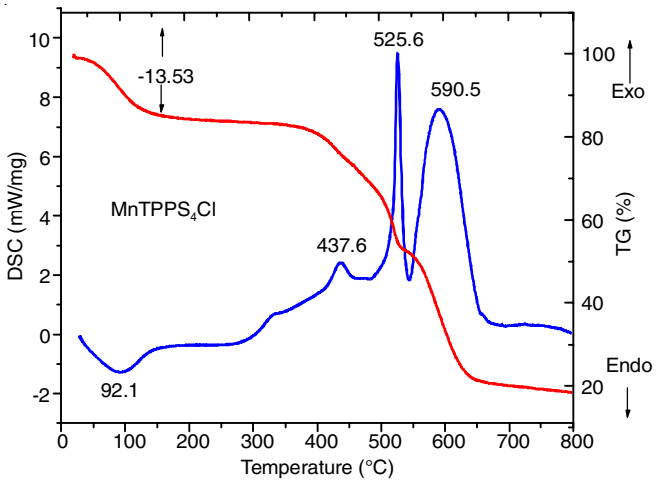

Fig. 8. TG/DSC curve for $MnTPPS_4Cl$

be formulated as $MnTPPS_4Cl{\cdot}10H_2O$. Thermal curve also shows total loss of 82% of metalloporphyrin including loss due to water. The DSC curve shows three decomposition temperatures at 437.6, 525.6 and 590.5 ºC, therefore, thermal stability of a compound is around up to 437 ºC. The residue after 800 ºC of $MnTPPS_4Cl$ exhibited 8.26% Na^+, 34.45% SO_4^{2-}, 50.42% coal and 6.36% metal oxide (Table-2).

First decomposition temperature and relative thermal stabilities of porphyrins: Thus, the first decomposition temperature of the porphyrin furnishes the information about its thermal stability. It is observed that $TPPS_4$ is thermally stable up to 361 ºC, $MnTPPS_4Cl$ at 437 ºC, $AgTPPS_4$ at 450 ºC and $CuTPPS_4$ up to 461 ºC (Fig. 9). In case of $TPPS_4$, a free-base porphyrin with no metal at the centre of the porphyrin ring, similarly, the vibrations between N and H at two sites make the ring comparatively unstable, $TPPS_4$, therefore, decomposes early. In $MnTPPS_4Cl$, when Mn^{3+} is introduced in the porphyrin hole, a perfect square pyramidal but ruffled structure is obtained. The Cl bonded to central Mn^{3+} ion is comparatively weak and it is lost first in the beginning of the TG/DSC event. This makes the compound to start the decomposition at 437 ºC. In $AgTPPS_4$ and $CuTPPS_4$, a nearly perfect square plane is observed because the ionic radii of Ag^{2+} and Cu^{2+} are 79 pm and 73 pm, respectively, which gives them nearly same stability. Thus, we see their (metalloporphyrins) decomposition temperatures are comparatively higher and make them more thermally stable. Fig. 10 gives the information about relative thermal stabilities of these porphyrins with reference to thermogravimetric curves. Therefore, the order of thermal stability for the above porphyrins can be given as:

$$CuTPPS_4 > AgTPPS_4 > MnTPPS_4Cl > TPPS_4$$

Conclusion

In conclusion, the aqueous free-base $TPPS_4$ and metalloporphyrins such as $CuTPPS_4$, $AgTPPS_4$ and $MnTPPS_4Cl$ were synthesized and characterized for their thermal studies. The synthesized porphyrins were nearly deliquescent in nature, therefore, using this property the number of molecules of water of crystallization for each compound were confirmed as $TPPS_4{\cdot}5H_2O$, $CuTPPS_4{\cdot}10H_2O$, $AgTPPS_4{\cdot}10H_2O$ and $MnTPPS_4Cl{\cdot}10H_2O$. The TG/DSC measurements conducted from room temperature to 800 ºC were used to determine the total loss of a substance, its decomposition temperature and ultimately the thermal stability of each porphyrin. Thus, the order of thermal stability is given as $CuTPPS_4 > AgTPPS_4 > MnTPPS_4Cl > TPPS_4$.

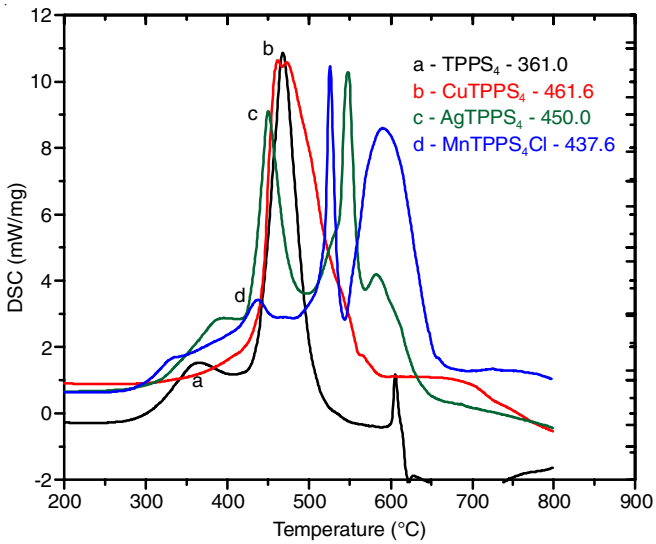

Fig. 9. First decomposition temperature for selected porphyrins

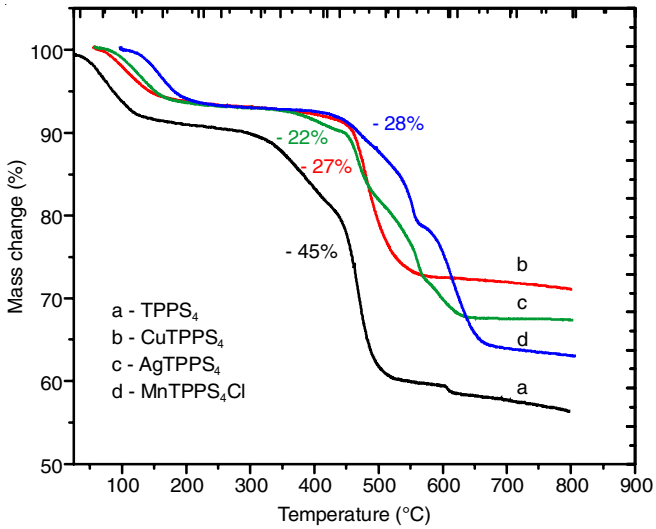

Fig. 10. Relative thermal stabilities of selected porphyrins

ACKNOWLEDGEMENTS

The authors are grateful to UGC-New Delhi for partial financial support for this investigation.

CONFLICT OF INTEREST

The authors declare that there is no conflict of interests regarding the publication of this article.

REFERENCES

1. M. Imran, M. Ramzan, A.K. Qureshi, M.A. Khan and M. Tariq, *Biosensors*, **8**, 95 (2018); https://doi.org/10.3390/bios8040095
2. S.V. Jenkins, A. Srivatsan, K.Y. Reynolds, F. Gao, Y. Zhang, C.D. Heyes, R.K. Pandey and J. Chen, *J. Colloid Interface Sci.*, **461**, 225 (2016); https://doi.org/10.1016/j.jcis.2015.09.037

3. H. Huang, W. Song, J. Rieffel and J.F. Lovell, *Front. Phys.*, **3**, 23 (2015); https://doi.org/10.3389/fphy.2015.00023
4. R.C. Huxford, J.D. Rocca and W. Lin, *Curr. Opin. Chem. Biol.*, **14**, 262 (2010); https://doi.org/10.1016/j.cbpa.2009.12.012
5. Y.N. Xue, Z.Z. Huang, J.T. Zhang, M. Liu, M. Zhang, S.W. Huang and R.X. Zhuo, *Polymer*, **50**, 3706 (2009); https://doi.org/10.1016/j.polymer.2009.05.033
6. S. De Robertis, M.C. Bonferoni, L. Elviri, G. Sandri, C. Caramella and R. Bettini, *Expert Opin. Drug Deliv.*, **12**, 441 (2015); https://doi.org/10.1517/17425247.2015.966685
7. W. Cheng, I.E. Haedicke, J. Nofiele, F. Martinez, K. Beera, T.J. Scholl, H.-L.M. Cheng and X. Zhang, *J. Med. Chem.*, **57**, 516 (2014); https://doi.org/10.1021/jm401124b
8. F. Hammerer, G. Garcia, S. Chen, F. Poyer, C. Fiorini-Debuisschert, S. Achelle, M.-P. Teulade-Fichou and P. Maillard, *J. Org. Chem.*, **79**, 1406 (2014); https://doi.org/10.1021/jo402658h
9. X. Dong, H. Chen, J. Qin, C. Wei, J. Liang, T. Liu, D. Kong and F. Lv, *Drug Deliv.*, **24**, 641 (2017); https://doi.org/10.1080/10717544.2017.1289570
10. A.S. Stender, K. Marchuk, C. Liu, S. Sander, M.W. Meyer, E.A. Smith, B. Neupane, G. Wang, J. Li, J.-X. Cheng, B. Huang and N. Fang, *Chem. Rev.*, **113**, 2469 (2013); https://doi.org/10.1021/cr300336e
11. M. Kueny-Stotz, A. Garofalo and D. Felder-Flesch, *Eur. J. Inorg. Chem.*, **2012**, 1987 (2012); https://doi.org/10.1002/ejic.201101163
12. H. Benveniste and S. Blackband, *Prog. Neurobiol.*, **67**, 393 (2002); https://doi.org/10.1016/S0301-0082(02)00020-5
13. H. Hummel, V.U. Weiler and R. Hoffmann, Targeting Contrast Agents or Targeting Therapeutic Agents for Molecular Imaging and Therapy, US Patent US20090238767A1 (2009).
14. L.M. Manus, R.C. Strauch, A.H. Hung, A.L. Eckermann and T.J. Meade, *Anal. Chem.*, **84**, 6278 (2012); https://doi.org/10.1021/ac300527z
15. A.S. Merbach, The Chemistry of Contrast Agents in Medical Magnetic Resonance Imaging; John Wiley & Sons: Hoboken, NJ, USA (2013).
16. F. Bryden and R.W. Boyle, Metalloporphyrins for Medical Imaging Applications. In Advances in Inorganic Chemistry; Elsevier: Amsterdam, The Netherlands; vol. 68, pp. 141 (2016).
17. J.C.P. Grancho, M.M. Pereira, M.D.G. Miguel, A.R. Gonsalves and H.D. Burrows, *Photochem. Photobiol.*, **75**, 249 (2002); https://doi.org/10.1562/0031-8655(2002)075<0249:SSAPOS>2.0.CO;2
18. S.K. Pandey, A.L. Gryshuk, A. Graham, K. Ohkubo, S. Fukuzumi, M.P. Dobhal, G. Zheng, Z. Ou, R. Zhan, K.M. Kadish, A. Oseroff, S. Ramaprasad and R.K. Pandey, *Tetrahedron*, **59**, 10059 (2003); https://doi.org/10.1016/j.tet.2003.10.016
19. A. Jemal, M.M. Center, C. DeSantis and E.M. Ward, *Cancer Epidemiol. Prev. Biomark.*, **20**, 1055 (2010); https://doi.org/10.1158/1055-9965.EPI-10-0437
20. M.J. Akhtar, M. Ahamed, H.A. Alhadlaq, S.A. Alrokayan and S. Kumar, *Clin. Chim. Acta*, **436**, 78 (2014); https://doi.org/10.1016/j.cca.2014.05.004
21. P. Zhang, C. Hu, W. Ran, J. Meng, Q. Yin and Y. Li, *Theranostics*, **6**, 948 (2016); https://doi.org/10.7150/thno.15217
22. J. Zhang, C. Jiang, J.P. Figueiró-Longo, R.B. Azevedo, H. Zhang and L.A. Muehlmann, *Acta Pharm. Sin. B*, **8**, 137 (2018); https://doi.org/10.1016/j.apsb.2017.09.003
23. M.A. Rajora, J.W.H. Lou and G. Zheng, *Chem. Soc. Rev.*, **46**, 6433 (2017); https://doi.org/10.1039/C7CS00525C
24. C.M. Lemon, E. Karnas, X. Han, O.T. Bruns, T.J. Kempa, D. Fukumura, M.G. Bawendi, R.K. Jain, D.G. Duda and D.G. Nocera, *J. Am. Chem. Soc.*, **137**, 9832 (2015); https://doi.org/10.1021/jacs.5b04765
25. A.A. Ptaszyñska, M. Trytek, G. Borsuk, K. Buczek, K. Rybicka-Jasiñska and D. Gryko, *Sci. Rep.*, **8**, 5523 (2018); https://doi.org/10.1038/s41598-018-23678-8
26. A.V. Salker and S.D. Gokakakar, *Int. J. Phys. Sci.*, **4**, 377 (2009).
27. S.D. Gokakakar and A.V. Salker, *Indian J. Chem. Technol.*, **16**, 492 (2009).
28. G. de la Torre, G. Bottari, M. Sekita, A. Hausmann, D.M. Guldi and T. Torres, *Chem. Soc. Rev.*, **42**, 8049 (2013); https://doi.org/10.1039/c3cs60140d
29. S. Saito and A. Osuka, *Angew. Chem. Int. Ed.*, **50**, 4342 (2011); https://doi.org/10.1002/anie.201003909
30. T.S. Srivastava and M. Tsutsui, *J. Org. Chem.*, **38**, 2103 (1973); https://doi.org/10.1021/jo00951a036
31. E.B. Fleischer, J.M. Palmer, T.S. Srivastava and A. Chatterjee, *J. Am. Chem. Soc.*, **93**, 3162 (1971); https://doi.org/10.1021/ja00742a012
32. W. De W. Horrocks Jr. and E.G. Hove, *J. Am. Chem. Soc.*, **100**, 4386 (1978); https://doi.org/10.1021/ja00482a012
33. F.R. Hopf and D.G. Whitten, in: K.M. Smith, Porphyrins and Metalloporphyrins, Elsevier, Amsterdam, Chap. 16, pp. 667 (1975).
34. S.D. Gokakakar and A.V. Salker, *J. Therm. Anal. Calorim.*, **109**, 1487 (2012); https://doi.org/10.1007/s10973-011-1952-4